# Investigation of the pharmacophore space of Severe Acute Respiratory Syndrome coronavirus (SARS-CoV) NTPase/helicase by dihydroxychromone derivatives

Chaewoon Lee [a,†], Jin Moo Lee [b,†], Na-Ra Lee [b], Dong-Eun Kim [a], Yong-Joo Jeong [b,*], Youhoon Chong [a,*]

[a] Department of Bioscience & Biotechnology, Konkuk University, Seoul 143-701, Republic of Korea
[b] Department of Bio and Nanochemistry, Kookmin University, Seoul 136-702, Republic of Korea

ABSTRACT

Aryl diketoacids have been identified as the first SARS-CoV NTPase/helicase inhibitors with a distinct pharmacophore featuring an arylmethyl group attached to a diketoacid. In order to search for the pharmacophore space around the diketoacid core, three classes of dihydroxychromone derivatives were prepared. Based on SAR study, an extended feature of the pharmacophore model of SARS-CoV NTPase/helicase was proposed which is constituted of a diketoacid core, a hydrophobic arylmethyl substituent, and a free catechol unit.

© 2009 Elsevier Ltd. All rights reserved.

In 2002, SARS (Severe Acute Respiratory Syndrome) caused by coronavirus (SARS-CoV) quickly spread to nearly 30 countries leading to infection over 8000 people, and almost 800 deaths worldwide.[1] Although new cases of the infection have not been reported since 2004, SARS remains as a global health threat due to its high mortality and lack of therapeutic agents.[2]

In our previous study,[3] we have identified aryl diketoacids (ADKs) as novel anti-SARS agents with selective inhibition (IC$_{50}$ = 5.4–13.6 μM) against duplex DNA-unwinding activity of SARS-CoV NTPase/helicase without significant impact on the ATPase activity. It is of particular interest that, among the SARS-CoV NTPase/helicase inhibitors reported to date,[3,4] ADK is the only example with distinct structure–activity relationship to provide an initial feature of the pharmacophore model composed of a diketoacid core with an appropriately positioned arylmethyl substituent (1, Fig. 1).

In this study, as a part of our ongoing efforts to delineate a complete pharmacophore model via structural variation on ADK, we designed several dihydroxychromone derivatives as a bioisostere of ADK in which the diketoacid moiety of ADK with poor drug-like property is replaced with a dihydroxychromone scaffold (Fig. 1). Dihydroxychromones, a class of naturally-occurring flavonoids

with proven stability and safety,[5] share the similar structural motif to the diketoacid of an ADK: two phenolic hydroxyl groups and a carbonyl oxygen serve together as an excellent mimic for the diketoacid functionality (Fig. 1). In addition, compared with an ADK with substituents attached only on one side of the diketoacid, various functionalities can be introduced to both sides of the dihydroxychromone core to allow extended investigation of the pharmacophore space. Thus, we designed novel dihydroxychromone derivatives with an arylmethyl functionality shown to play a critical role in inhibitory activity of ADKs[3] as well as a catechol moiety known to be responsible for various biological activities of flavonols[6] on either side (2 and 3, Fig. 2) or both sides (4, Fig. 2) of the dihydroxychromone scaffold. Herein, we present a
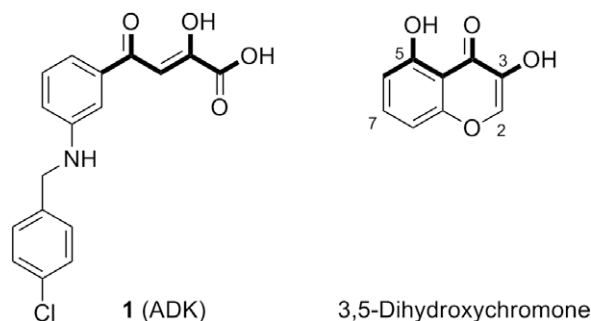


Figure 1. Comparison of ADK and dihydroxychromone.

* Corresponding authors. Tel.: +82 2 910 5454; fax: +82 2 910 4415 (Y.-J.J.); tel.: +82 2 2049 6100; fax: +82 2 454 8217 (Y.C.).
E-mail addresses: jeongyj@kookmin.ac.kr (Y.-J. Jeong), chongy@konkuk.ac.kr (Y. Chong).
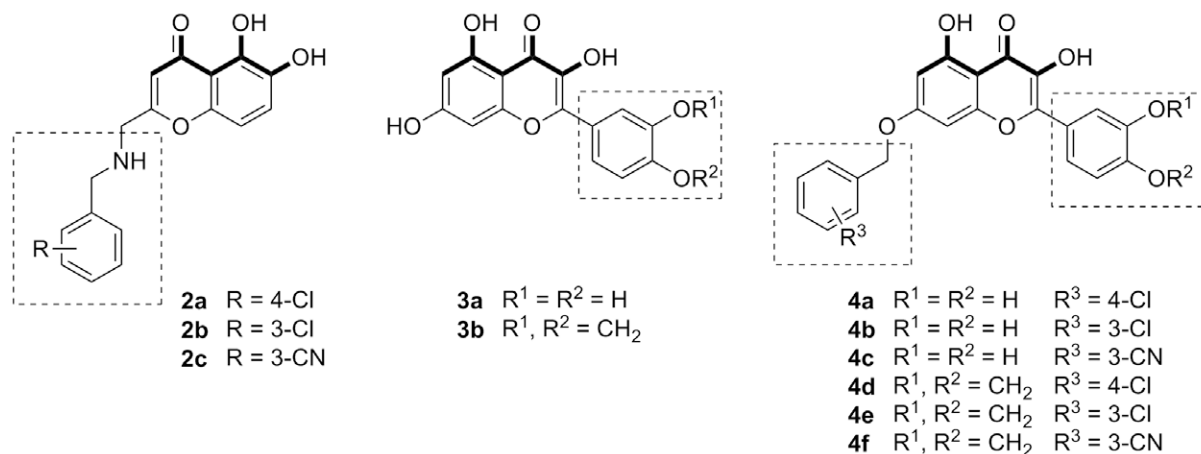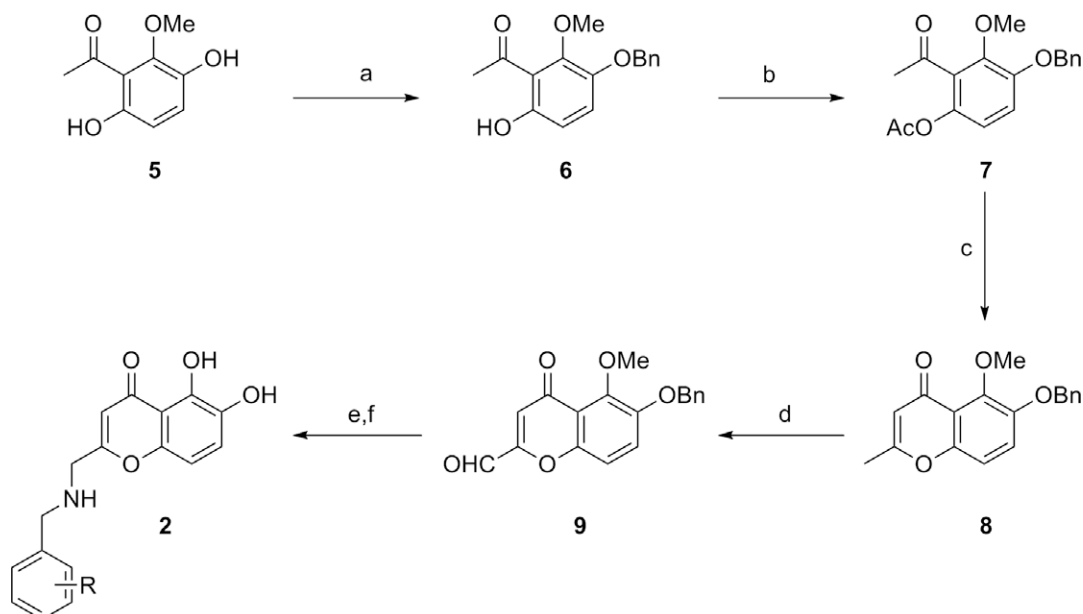† These two authors contributed equally to this work.

**Figure 2.** Design of dihydroxychromone derivatives with mono- (**2** and **3**) and di-substituents (**4**) on the dihydroxychromone scaffold.



**Scheme 1.** Syntheses of 2-[N-(arylmethyl)methyl]-5,6-dihydroxy chromone derivatives (**2a**: R = 4-Cl, **2b**: R = 3-Cl, **2c**: R = 3-CN). Reagents and conditions: BnBr, $K_2CO_3$, acetone, 60 °C; (b) AcCl, Pyr, 60 °C; (c) LiHMDS, THF, −78 °C; (d) SeO_2, bromobenzene, 160 °C; (e) (R-Ph)CH_2NH_2, AcOH, MeOH, NaBH_3CN, rt; (f) BBr_3, CH_2Cl_2, rt.

novel pharmacophore model of SARS-CoV NTPase/helicase inhibitors via syntheses and biological evaluation of three classes of dihydroxychromone derivatives.
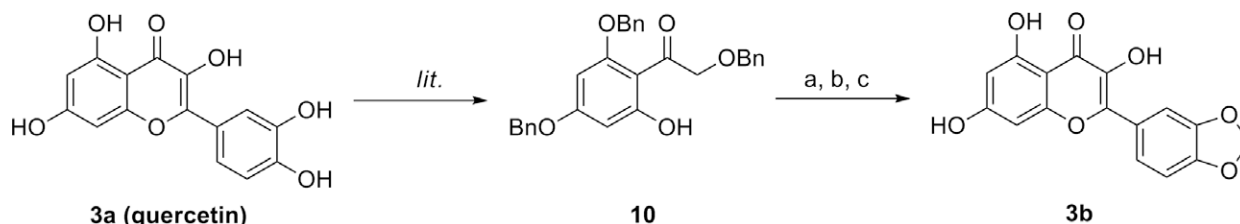
2-[N-(Arylmethylamino)methyl]-5,6-dihydroxychromones (**2**, Fig. 2) superimposable to ADK were prepared starting from acetophenone **5** (Scheme 1).[7] Regioselective benzylation of **5**[8] followed by acetylation provided the fully protected acetophenone **7** (71% yield for two steps), which underwent cyclization (48% yield) and subsequent oxidation to give the aldehyde **9** in 91% yield. The desired dihydroxychromone derivatives **2a–2c** were prepared from the intermediate **9** by reductive amination followed by deprotection with BBr_3 in CH_2Cl_2 (31–38% yield).

Free or protected catechol was introduced at the other side of the dihydrochromone to give flavonol derivatives (**3**, Scheme 2). The free catechol derivative [quercetin (**3a**)] was obtained from commercial source and the 3,6-dihydroxychromone derivative with protected catechol functionality at 2 position (**3b**) was synthesized starting from the phenol **10** which was
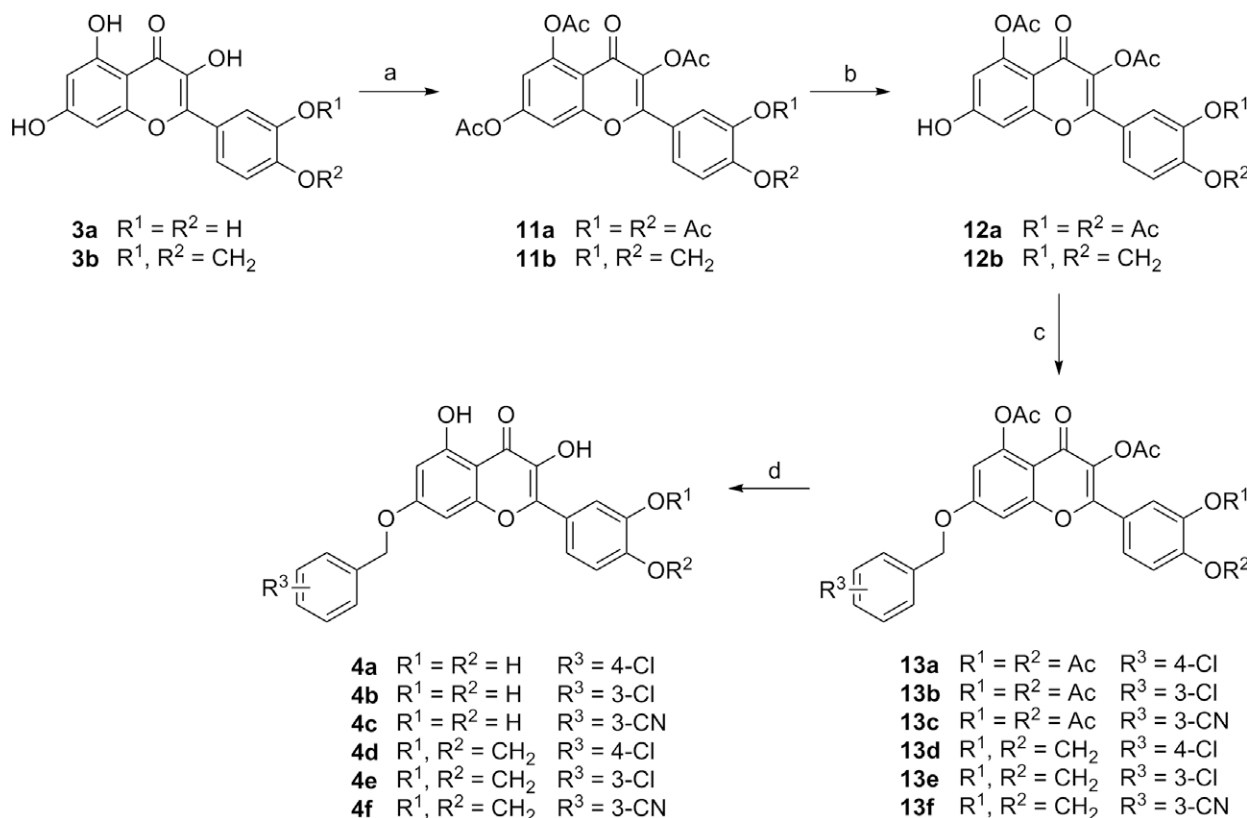
prepared by degradation of pentabenzylated quercetin[9] (65% yield, Scheme 2). Esterification of phenol **10** with piperonyloyl chloride gave the corresponding ester. Cyclization of the ester in the presence of $K_2CO_3$ and phase transfer catalyst,[10] followed by hydrogenolysis provided the flavonol **3b** (72% yield for two steps).

Synthesis of dihydroxychromones with substituents on both sides (**4**) was accomplished by selective alkylation on 7-O position of the flavonol (**3a** and **3b**) (Scheme 3). Thus, peracetylation of **3a** (or **3b**) followed by selective deacetylation of 7-OAc with thiophenol and imidazole in NMP at 0 °C gave the 7-O-mono deprotected flavonol **12a** (or **12b**).[11] Treatment of **12a** (or **12b**) with substituted benzyl bromide in acetone in the presence of $K_2CO_3$ at room temperature, followed by methanolysis provided the desired compounds **4a–4f** in 25–29% yields.

The synthesized dihydroxychromone derivatives[12] were tested for their inhibitory activities against ATPase and duplex DNA-unwinding activities of the helicase by phosphate release assay[13]

**Scheme 2.** Syntheses of **3b** from commercially available **3a** (quercetin). Reagents and conditions: (a) piperonyloyl chloride, Pyr; (b) K₂CO₃, TBAB, toulene, 90 °C; (c) H₂, Pd/C, MeOH/CH₂Cl₂.



**Scheme 3.** Syntheses of dihydrochromone derivatives with substituents on both sides of the core diketoacid mimic. Reagents and conditions: Ac₂O, Pyr; (b) PhSH, imidazole, NMP, 0 °C, rt; (c) (R³-Ph)CH₂Br, K₂CO₃, acetone, rt; (d) NH₃/MeOH, rt.

and FRET-based assay,[14] respectively. Cloning and purification of the SARS-CoV helicase were performed as previously described.[15]

Like ADK analogues,[3] dihydroxychromone derivatives showed no significant inhibition against helicase ATPase activity. Only marginal inhibition of the ATPase activity (20.9 and 25.4 μM) was observed with two disubstituted dihydroxychromone derivatives (**4a** and **4c**, Table 1). Unexpectedly, compounds **2a**–**2c**, superimposable to the ADK scaffold inhibited neither ATPase nor duplex DNA-unwinding activity of SARS-CoV ATPase/helicase. Presumably, the high flexibility of (N-arylmethyl)methyl substituent of **2a**–**2c** compared with the ADK counterpart resulted in loss of inhibitory activity.

A flavonol with protected catechol group (**3b**) also failed to show any inhibition against ATPase/helicase. However, a flavonol with free catechol (quercetin, **3a**) selectively inhibited the duplex DNA-unwinding activity in micromolar range (IC₅₀ = 8.1 μM, Table 1) to indicate the possible role of the free catechol moiety in the binding interaction with the target enzyme presumably as a hydrogen bond donor.
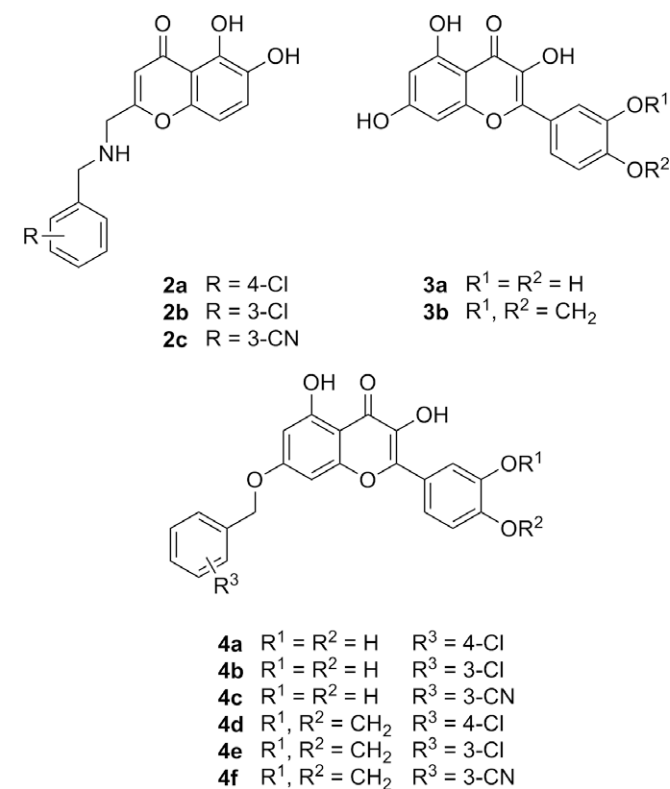
Interestingly, substitution of arylmethyl functionality on 7-O position of **3b** remarkably increased the activity of the resulting compounds (**4d**–**4f**, Table 1). The inhibitory activity of quercetin (**3a**) was also improved upon introduction of arylmethyl substituent at 7-O position (**4a**–**4c**, Table 1). It is noteworthy that flavonol derivatives with free catechol moieties (**4a**–**4c**) are usually two to three times more active than the protected catechol counterparts (**4d**–**4f**). The synergistic effect of the two substituents attached to the opposite side of the dihydrochromone core suggests the presence of two distinct binding sites on the target enzyme: a hydrophobic arylmethyl binding site and a catechol binding site capable of hydrogen bonding interaction.

On the basis of this study, we hypothesize an extended pharmacophore model (Fig. 3) of SARS-CoV NTPase/helicase inhibitors composed of three key components including a diketoacid core, a hydrophobic site and a free catechol moiety.
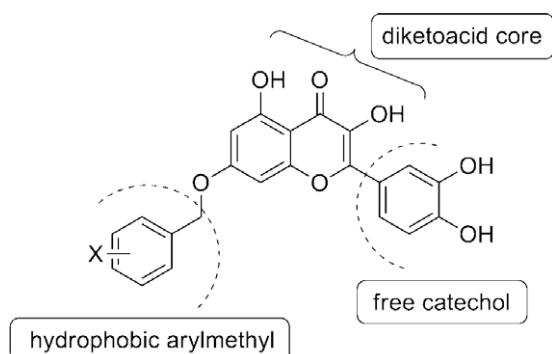
In summary, in order to investigate the pharmacophore space around the diketoacid core of SARS-CoV NTPase/helicase inhibitors, three classes of dihydroxychromone derivatives were prepared in

**Table 1**
IC$_{50}$ values of flavonol derivatives against SARS-CoV helicase ATPase activity and duplex DNA-unwinding activity



**2a** R = 4-Cl  **3a** R$^1$ = R$^2$ = H
**2b** R = 3-Cl  **3b** R$^1$, R$^2$ = CH$_2$
**2c** R = 3-CN

**4a** R$^1$ = R$^2$ = H   R$^3$ = 4-Cl
**4b** R$^1$ = R$^2$ = H   R$^3$ = 3-Cl
**4c** R$^1$ = R$^2$ = H   R$^3$ = 3-CN
**4d** R$^1$, R$^2$ = CH$_2$   R$^3$ = 4-Cl
**4e** R$^1$, R$^2$ = CH$_2$   R$^3$ = 3-Cl
**4f** R$^1$, R$^2$ = CH$_2$   R$^3$ = 3-CN

| Compds | IC$_{50}$ (μM) | |
|---|---|---|
| | ATPase | Duplex DNA-unwinding |
| **2a** | >50 | >50 |
| **2b** | >50 | >50 |
| **2c** | >50 | >50 |
| **3a** | >50 | 8.1 ± 0.3 |
| **3b** | >50 | >50 |
| **4a** | 20.9 ± 0.5 | 4.1 ± 0.3 |
| **4b** | >50 | 5.2 ± 0.4 |
| **4c** | 25.4 ± 1.5 | 2.7 ± 0.1 |
| **4d** | >50 | 9.3 ± 0.4 |
| **4e** | >50 | 15.4 ± 0.8 |
| **4f** | 42.9 ± 5.4 | 8.1 ± 0.3 |

which two different substituents, arylmethyl and catechol, are attached on opposite ends. The synthesized dihydroxychromones showed selective inhibition against duplex DNA-unwinding activity of SARS-CoV NTPase/helicase. Moreover, the inhibitory activity was enhanced by combination of the two spatially separated substituents, which indicates two different binding sites in the target enzyme. Taken together, an extended feature of the pharmacophore model was proposed which is constituted of a diketoacid core, a hydrophobic arylmethyl substituent, and a free catechol unit. Further structure–activity study around the proposed pharmacophore model is warranted for discovery of more potent inhibitors of SARS-CoV NTPase/helicase.

## Acknowledgments

## Supplementary data

Supplementary data associated with this article can be found, in the online version, at doi:10.1016/j.bmcl.2009.07.009.

## References and notes

1. (a) Peiris, J. S.; Lai, S. T.; Poon, L. L.; Guan, Y.; Yam, L. Y.; Lim, W.; Nicholls, J.; Yee, W. K.; Yan, W. W.; Cheung, M. T.; Cheng, V. C.; Chan, K. H.; Tsang, D. N.; Yung, R. W.; Ng, T. K. Lancet 2003, 361, 1319; (b) Drosten, C.; Gunther, S.; Preiser, W.; van der Werf, S.; Brodt, H. R.; Becker, S.; Rabenau, H.; Panning, M.; Kolesnikova, L.; Fouchier, R. A.; Berger, A.; Burguiere, A. M.; Cinatl, J.; Eickmann, M.; Escriou, N. N. Engl. J. Med. 2003, 348, 1967.
2. http://www.who.int/csr/sars/en.
3. Lee, C.; Lee, J. M.; Lee, N. R.; Jin, B. S.; Jang, K. J.; Kim, D. E.; Jeong, Y. J.; Chong, Y. Bioorg. Med. Chem. Lett. 2009, 19, 1636.
4. (a) Kliger, Y.; Levanon, E. Y.; Gerber, D. Drug Discovery Today 2005, 10, 345; (b) Yang, N.; Tanner, J. A.; Wang, Z.; Huang, J. D.; Zheng, B. J.; Zhu, N.; Sun, H. Chem. Commun. 2007, 4413; (c) Kesel, A. J. Anti-Infective Agents Med. Chem. 2006, 5, 161.
5. Spedding, G.; Ratty, A.; Middleton, E., Jr. Antiviral Res. 1989, 12, 99.
6. (a) Morel, I.; Lescoat, G.; Cogrel, P.; Sergent, O.; Pasdeloup, N.; Brissot, P.; Cillard, P.; Cillard, J. Biochem. Pharmacol. 1993, 4, 13; (b) Van Acker, S. A. B. E.; Van den Berg, D. J.; Tromp, M. N. J. L.; Griffoen, D. H.; van Bennekom, W. P.; van der Vijjgh, W. J. F.; Bast, A. Free Radical Biol. Med. 1996, 20, 331; (c) Chiang, L. C.; Chiang, W.; Liu, M. C.; Lin, C. C. J. Antimicrob. Chmother. 2003, 52, 194; (d) Formica, J. V.; Regelson, W. Food Chem. Toxicol. 1995, 33, 1061.
7. Prakash, O.; Pundeer, R.; Kaur, H. Synthesis 2003, 18, 2768.
8. Wollenweber, E.; Iinuma, M.; Tanaka, T.; Mizuno, M. Phytochemistry 1990, 29, 633.
9. Hauteville, M.; Chadenson, M.; Chopin, J. Bull. Soc. Chim. Fr. 1979, 11, 124.
10. Caldwell, S. T.; Petersson, H. M.; Farrugia, L. J.; Mullen, W.; Crozier, A.; Hartley, R. C. Tetrahedron 2006, 62, 7257.
11. Li, M.; Han, X.; Yu, B. J. Org. Chem. 2003, 68, 6842.
12. See Supplementary data for experimental and characterization data for the final compounds (2a–2c, 3b, and 4a–4f) as well as previously unreported intermediates.
13. (a) Baykov, A. A.; Evtushenko, O. A.; Avaeva, S. M. Anal. Biochem. 1988, 171, 266; (b) Wardell, A. D.; Errington, W.; Ciaramella, G.; Merson, J.; McGarvey, M. J. J. Gen. Virol. 1999, 80, 701; (c) Martin, G. R.; Yvette, M. N.; Chrisotomos, P.; Laurence, H. P.; Paul, W.; Wynne, A. Anal. Biochem. 2004, 327, 176.
14. Jang, K. J.; Lee, N. R.; Yeo, W. S.; Jeong, Y. J.; Kim, D. E. Biochem. Biophys. Res. Commun. 2008, 366, 738.
15. Yang, N.; Tanner, J. A.; Wang, Z.; Huang, J. D.; Zheng, B. J.; Zhu, N.; Zun, H. Chem. Commun. 2007, 4413.



**Figure 3.** The proposed pharmacophore model of SARS-CoV helicase inhibitors.